

Induction of Caspase-8 and Death Receptors by a New Dammarane Skeleton from the Dried Fruits of *Forsythia koreana*

Usama W. Hawas^{a,b,*}, Amira M. Gamal-Eldeen^{c,*}, Samy K. El-Desouky^a, Young-Kyoon Kim^d, Antje Huefner^e, and Robert Saf^f

^a Phytochemistry and Plant Systematic Department, National Research Center, Dokki 12622, Cairo, Egypt. Fax: +202 3370931. E-mail: hawasusama@yahoo.com

^b Marine Chemistry Department, Faculty of Marine Sciences, King Abdulaziz University, Jeddah 21589, KSA

^c Cancer Biology Laboratory, Center of Excellence for Science, National Research Center, Dokki 12622, Cairo, Egypt. Fax: +202 33370931. E-mail: aeldeen7@yahoo.com

^d College of Forest Science, Kookmin University, Seoul, 136-702, Korea

^e Pharmaceutical Sciences Institute, Pharmaceutical Chemistry Department, University of Graz, A-8010 Graz, Austria

^f Institute of Chemical Technology of Organic Materials, Erzherzog-Johann University, A-8010 Graz, Austria

* Authors for correspondence and reprint requests

Z. Naturforsch. **68c**, 29–38 (2013); received August 26, 2011/October 29, 2012

A new naturally occurring compound based on the dammarane skeleton, *i.e.* cabralealactone 3-acetate-24-methyl ether, was isolated from the aqueous methanolic extract of *Forsythia koreana* fruits, along with eight known compounds: cabralealactone 3-acetate, ursolic acid, arctigenin, arctiin, phillyrin, rutin, caffeic acid, and rosmarinic acid. The identification of the isolated compounds was based on their spectral analysis including: HREI-MS, 1D and 2D NMR spectroscopy. The selected compounds and the aqueous methanolic extract were evaluated for their cytotoxic activity against human solid tumour cell lines. Cabralealactone 3-acetate-24-methyl ether and ursolic acid were found to be active against human breast cancer cells (MCF-7). The cytotoxicity was associated with the activation of caspase-8, the induction of the death receptors DR4 and DR5, as well as DNA fragmentation, and was thus due to apoptosis rather than necrosis.

Key words: *Forsythia koreana*, Dammarane, Breast Cancer

Introduction

Naturally occurring compounds have given rise to approximately half of all pharmaceuticals introduced to the market over the past 20 years (Vuorela *et al.*, 2004). The Oleaceae, the olive family, is a plant family containing 24 extant genera and around 600 species of mesophytic shrubs, trees, and occasionally vines (Bae, 2000).

The dried fruits of one of its members, *Forsythia koreana*, have long been used in Chinese medicine as therapeutic agents for the treatment of infectious and inflammatory disorders, as well as lung bronchiolitis, tonsillitis, sore throat, fever, vomiting, heart disease, HIV/AIDS, gonorrhea, pain, and skin rash (Lee *et al.*, 1996). Sometimes the extract of forsythia is given intravenously in combination with other herbs for treating bronchiolitis (Kong *et al.*, 1993). The fruits of *F. koreana* are also known to have diuretic, antibacterial, anti-inflammatory,

and damp-heat clearing actions, and have been used for the treatment of dysuria, edema, urinary tract infection, and retention of fluid in Oriental traditional medicine (Kitagawa *et al.*, 1984a, 1987; Kong *et al.*, 1993; Kim *et al.*, 2000; Lee *et al.*, 2010).

In previous investigations, the methanolic extract of *F. koreana* fruits was found to inhibit the release of histamine, TNF- α , IL-6, and IL-8 from mast cells (Choi *et al.*, 2007). Aqueous extracts of *F. forsythiae* were found to block the activity of the initiator caspase-8, as well as the effectors caspase-3 and caspase-7 in a dose-dependent manner with an IC₅₀ value of 10 μ g/ml (Fattorusso *et al.*, 2006). Previous phytochemical studies have revealed the presence of various biologically active ingredients in *F. koreana* including: lignans, flavonoids, caffeoyl glucosides, and terpenes (Kitagawa *et al.*, 1984a; Nishibe, 2002; El-Desouky and Kim, 2008; Kim and Lee, 2009; Lee *et al.*, 2010; Jung *et al.*, 2010). The *n*-butanol fraction of *F. koreana* fruits inhibited NO

production, due to the suppression of iNOS gene expression, in RAW 264.7 cells stimulated with interferon- γ (IFN- γ) and lipopolysaccharide (LPS) (Kitagawa *et al.*, 1984b; Kim *et al.*, 2000).

In the present work, we have investigated the phytochemicals in the aqueous methanolic extract of *F. koreana* fruits and explored the antitumour activity of some of them.

Results and Discussion

The ethyl acetate fraction from the aqueous methanolic extract of the dried fruits of *F. koreana* was subjected to a combination of column and preparative silica gel chromatography to afford the two dammarane skeleton compounds **1** and **2**, as well as ursolic acid (**3**) (Fig. 1), a known triterpenoid compound (Seebacher *et al.*, 2003).

Characterization of cabralealactone 3-acetate (**2**) and its methyl ether **1**

Compound **2** was obtained as a white powder with $[\alpha]_D^{25}$ of $+46^\circ$ (*c* 0.1, CHCl_3) and an $[\text{M}+\text{Na}]^+$

peak in the +ESI-mass spectrum at m/z 469, and identified by 1D and 2D NMR spectroscopy as cabralealactone 3-acetate; it was previously isolated from *Cabralea eichleriana* as cabraleahydroxylactone and purified only as its acetate (Rao *et al.*, 1975).

Compound **1** was obtained as a white powder, $[\alpha]_D^{25}$ $+82^\circ$ (*c* 0.1, CHCl_3), and the HREI-mass spectrum gave an $[\text{M}]^+$ peak at m/z 474 corresponding to the molecular formula $\text{C}_{30}\text{H}_{50}\text{O}_4$, suggesting six double-bond equivalents in the molecule. The ^1H NMR spectra of **1** and **2** (Table I) showed similar features except for the presence of a singlet at δ_{H} 3.32 ppm assigned to the methoxy group of **1**. The ^1H NMR spectrum of **1** also showed eight tertiary methyl singlets, an acetyl group at δ_{H} 2.05 ppm, two oxymethine protons at δ_{H} 4.91 ppm (d, $J = 4.8$ Hz) and 4.48 ppm (dd, $J = 10.2, 5.9$ Hz), and a series of resolved and unresolved multiplets extending from δ_{H} 0.84 to 1.89 ppm.

The ^{13}C NMR spectrum of **1** (Table I) displayed 30 carbon atom resonances, while the

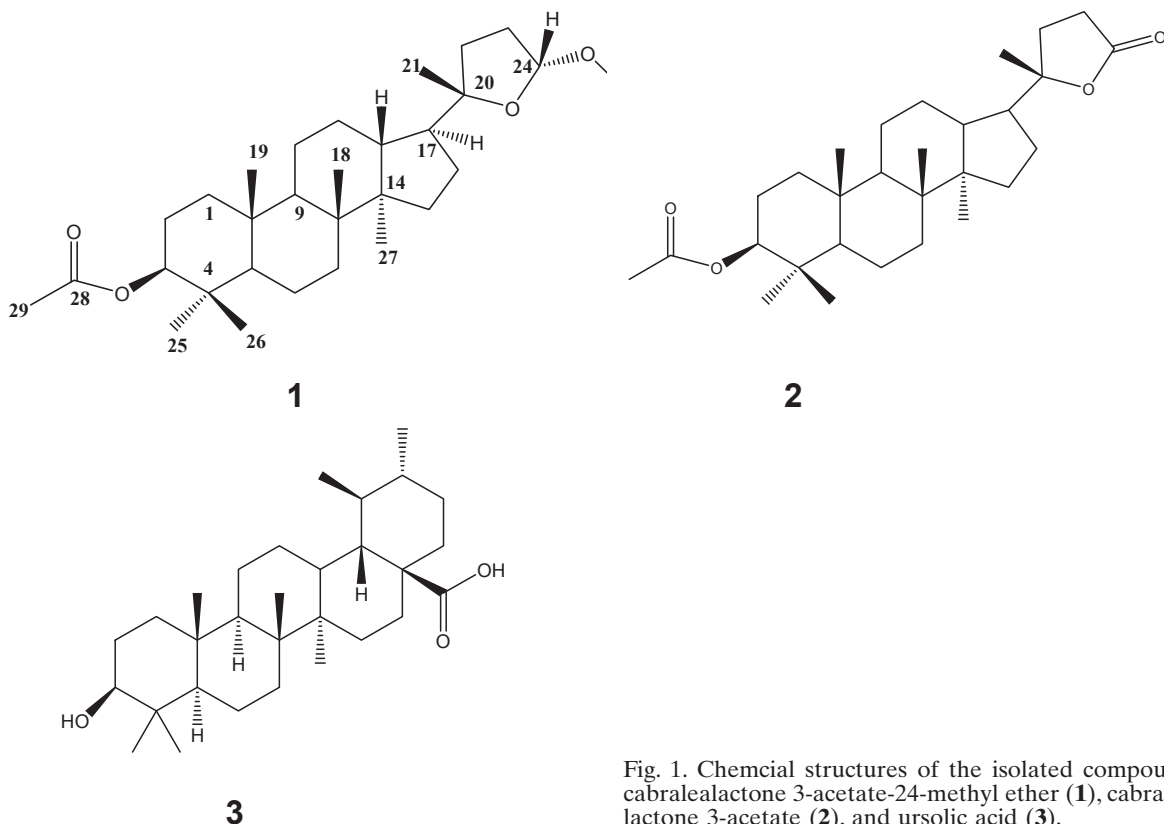


Fig. 1. Chemical structures of the isolated compounds cabralealactone 3-acetate-24-methyl ether (**1**), cabralealactone 3-acetate (**2**), and ursolic acid (**3**).

Table I. ^{13}C NMR (100.5 MHz) and ^1H NMR (400 MHz) data for cabralealactone 3-acetate (**2**) and **1** in CDCl_3 with shifts as δ values and coupling constants J in Hz.

Position	1			2		
	mult J	^1H	^{13}C	mult J	^1H	^{13}C
1	<i>m</i> <i>td</i> 4.0, 7.2	1.05 1.69	38.6	<i>d</i> 7.2 <i>td</i> 4.0, 7.2	1.00 1.64	38.5
2	<i>m</i>	1.64	23.6	<i>m</i>	1.63	23.5
3	<i>dd</i> 10.2, 5.9	4.48	81.0	<i>dd</i> 10.4, 5.7	4.48	80.7
4	-	-	37.7	-	-	37.8
5	<i>m</i>	0.84	55.9	<i>m</i>	0.84	55.8
6	<i>m</i> <i>m</i>	1.49 1.44	18.0	<i>m</i> <i>m</i>	1.52 1.45	18.1
7	<i>m</i> <i>m</i>	1.55 1.28	35.0	<i>m</i> <i>m</i>	1.26 1.53	35.1
8	-	-	40.2	-	-	40.3
9	<i>m</i>	1.36	51.0	<i>m</i>	1.34	50.2
10	-	-	37.0	-	-	36.9
11	<i>m</i> <i>m</i>	1.20 1.48	21.4	<i>m</i> <i>m</i>	1.23 1.52	21.3
12	<i>m</i> <i>m</i>	1.22 1.76	26.5	<i>m</i> <i>m</i>	1.24 1.75	26.6
13	<i>m</i>	1.60	43.4	<i>m</i>	1.58	43.1
14	-	-	50.5	-	-	50.4
15	<i>m</i> <i>m</i>	1.12 1.51	31.1	<i>m</i> <i>m</i>	1.07 1.49	31.1
16	<i>d</i> 4.8 <i>m</i>	1.82 1.64	25.3	<i>d</i> 4.8 <i>m</i>	1.83 1.37	24.9
17	<i>m</i>	1.86	50.0	<i>m</i>	1.96	49.2
18	<i>s</i>	0.96	15.4	<i>s</i>	0.96	15.4
19	<i>s</i>	0.88	16.2	<i>s</i>	0.88	16.1
20	-	-	88.0	-	-	90.0
21	<i>s</i>	1.11	23.4	<i>S</i>	1.36	25.3
22	<i>m</i> <i>m</i>	1.89 1.63	34.9	<i>dt</i> 12.7, 9.9 <i>m</i>	2.10 1.93	31.2
23	<i>m</i> <i>m</i>	2.05 1.89	32.6	<i>dt</i> 18.3, 9.7 <i>ddd</i> 18.3, 9.9, 4.3	2.64 2.55	29.2
24	<i>d</i> 4.8	4.91	104.5	-	-	176.7
25	<i>s</i>	0.86	16.2	<i>s</i>	0.87	16.2
26	<i>s</i>	0.84	27.8	<i>s</i>	0.86	27.9
27	<i>s</i>	0.85	16.4	<i>s</i>	0.86	16.4
28-COO	-	-	170.7	-	-	170.9
29	<i>s</i>	2.03	21.2	<i>s</i>	2.05	21.1
30-OCH ₃	<i>s</i>	3.32	54.4	-	-	-

HSQC experiment confirmed that 24 out of the 30 carbon atoms were attached to protons. The multiplicities of the carbon signals were determined by performing a DEPT experiment which revealed the presence of eight methyl groups, ten methylene groups, six methane groups, and six quaternary carbon atoms. Therefore, the unsaturation index exhibited by the molecular for-

mula of **1** was satisfied by the four rings of a dammarane skeleton, an ester carbonyl group (δ_{C} 170.7 ppm) and the cyclized side chain at C-17. The downfield resonance (δ_{H} 4.48 ppm) of one of the oxymethine protons in **2**, which was attached to a carbon atom at δ_{C} 81 ppm, suggested it to be esterified. The large coupling constants ($J = 10.2$ and 5.9 Hz) of this proton demonstrated the equatorial (β -)orientation of the acetyl moiety. In the HMBC spectrum (Table II), the proton at δ_{H} 4.48 ppm showed two bond correlations to δ_{C} 23.6 ppm (C-2) and 37.7 ppm (C-4), and connectivities over to 3J 38.6 ppm (C-1), 55.9 ppm (C-5), and the C-4 methyl groups at δ_{C} 16.2 and 27.9 ppm. These HMBC correlations defined the site of esterification at C-3.

In the ^{13}C NMR spectrum of **1**, the carbon signal of the carbonyl carbon atom of the γ -lactone at δ_{C} 176.7 ppm in cabralealactone 3-acetate (**2**) was chemically shifted upfield to δ_{C} 104.5 ppm and assigned as hemi-acetal methine group through the HSQC correlation between δ_{C} 104.5 ppm and δ_{H} 4.91 ppm. The location of this functionality at C-24 was confirmed by 3J HMBC correlations (Fig. 2)

Table II. Key HMBC correlations for **1**.

Proton	4J	3J	2J
H-1	C-8	C-3, C-5, C-9, C-19	C-2, C-10
H-2	C-5	C-4, C-10	C-1, C-3
H-3	C-10	C-1, C-5, 28-COO, C-25, C-2, C-4 C-26	
H-5		C-3, C-7	C-6
H-6		C-8, C-10	C-5
H-7		C-5, C-9	C-6, C-8
H-9	C-6	C-1, C-5, C-7, C-12, C-14	C-8
H-11	C-14	C-13	C-9, C-12
H-12		C-14	
H-13		C-13, C-20	C-14
H-15	C-20	C-8, C-13, C-17, C-27	C-16
H-16	C-22	C-13, C-20	C-15, C-17
H-17	C-23	C-12, C-14, C-22	C-13, C-16, C-20
H-18		C-8, C-9, C-14	C-7
H-19		C-1, C-5	C-10
H-21		C-17, C-23	C-20, C-22
H-22		C-24	C-20
H-23	C-21	C-20	C-22, C-24
H-24	C-17	C-20, C-22, 30-OCH ₃	C-23
H-25		C-3, C-5	C-4
H-26		C-3, C-5	C-4
H-27		C-11	C-14
H-29	C-3	C-3	28-COO
30-OCH ₃		C-24	

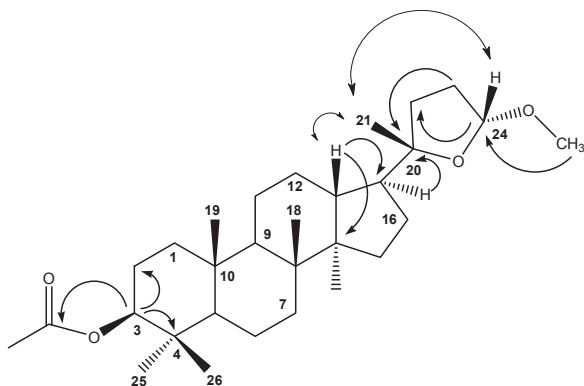


Fig. 2. Some selected HMBC (—) and NOE correlations of **1**.

from this proton to δ_C 88.0 ppm (C-20), 34.9 ppm (C-22), and 54.4 ppm (-OCH₃), as well as a 2J correlation with 32.6 ppm (C-23) and a 4J correlation with 50.0 ppm (C-17). The axial (α -) orientation of the hydroxy function at C-24 was determined from the coupling constant ($J = 4.8$ Hz) between H-24 β (equatorial) and H₂-23. The chemical shift and splitting pattern of the downfield oxymethine group (δ_H 4.91 ppm and δ_C 104.5 ppm) indicated that the group must be attached with two oxygen atoms (hemi-acetal group). The assignments of the remaining carbon signals in **2** were based on HMBC experiments using 3J in addition to 2J and 4J correlations from the methine and methyl group protons, respectively, to carbon atoms, while the $^1J_{C-H}$ interactions observed in the HSQC spectrum allowed unambiguous assignments of the methylene protons in **1**.

The relative stereochemistry of C-17 and the oxymethine at C-24 in **1** was finally determined by 1D NOE experiments, as indicated in the structure. Irradiation at the resonance frequency of H-24 produced strong enhancement of the methyl signals, H₃-21. On the other hand, similar irradiation of the H₃-21 signal showed significant enhancement of H-24, while the former one also showed enhancement of H-13, suggesting their close proximity. On the basis of the above spectral data, the structure of compound **1** was elucidated as cabralealactone 3-acetate-24-methyl ether, a new dammarane skeleton which has not been reported previously to occur in nature.

Evaluation of cytotoxicity and death mechanism

Cytotoxicity activity

Exploring the cytotoxic effect of different doses of the extract and of compounds **1**–**3** on the solid tumour cell lines Hep-G2, HCT-116, and MCF-7, in addition to normal rat splenocytes, using the 3-(4,5-dimethyl-2-thiazolyl)-2,5-diphenyl-2H-tetrazolium bromide (MTT) assay, *i.e.* an assay revealing metabolic cytotoxicity, indicated that all tested compounds possessed low cytotoxicity against Hep-G2 and HCT-116 cells ($IC_{50} > 20$ μ g/ml) in comparison to paclitaxel cytotoxicity, as shown in Table III. On the other hand, compound **1** was the most cytotoxic compound against MCF-7 cells ($IC_{50} = 6.46$ μ g/ml) and compound **3** was moderately cytotoxic ($IC_{50} = 18.25$ μ g/ml), thus revealing a promising anticancer activity against breast cancer. None of the tested samples possessed any cytotoxicity against normal rat splenocytes, which exhibited cell viability of 83.5% and 92.5% in the presence of the highest concentration tested.

DNA fragmentation

Cell death is generally classified into two categories: apoptosis, representing “active” programmed cell death, and necrosis, representing “passive” cell death without (known) underlying regulatory mechanisms; both are distinguished by well defined morphological and biochemical features. Necrosis is characterized by cell swelling, disruption, and rapid disintegration of the cell membrane (Kalka *et al.*, 2000). In contrast, during apoptosis the cells undergo nuclear and cytoplasmic shrinkage, chromatin condensation and fragmentation, and the cells are finally broken into multiple membrane-surrounded bodies (apoptotic bodies) (Vuorela *et al.*, 2004). Com-

Table III. Cytotoxicity (IC_{50} , μ g/ml) of test compounds against human malignant cell lines after 48 h of incubation.

Sample	Cell line		
	HCT-116	MCF-7	Hep-G2
Extract	> 50	> 50	> 50
1	31.10 \pm 1.94	6.46 \pm 1.37	29.63 \pm 0.17
2	> 50	49.06 \pm 3.37	> 50
3	45.20 \pm 4.18	18.25 \pm 1.94	37.91 \pm 1.11
Paclitaxel	0.41 \pm 0.13	0.97 \pm 0.20	0.49 \pm 0.10

pounds **1** and **3** were found to greatly enhance the degree of DNA fragmentation, which was assayed using diphenylamine, compound **1** being the more potent DNA-damaging agent (Fig. 3A).

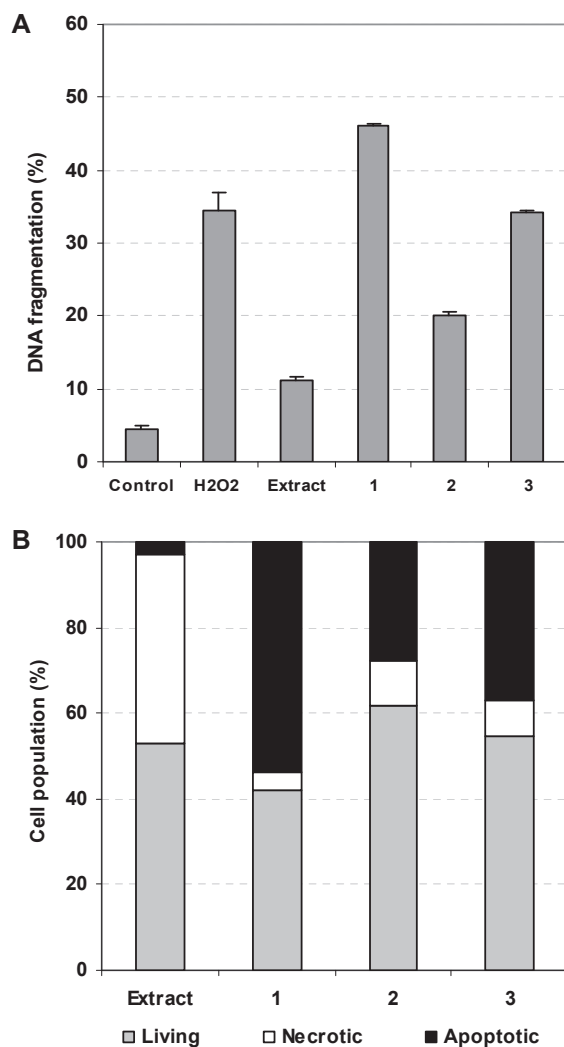


Fig. 3. (A) The effect of test compounds on the percentage of DNA fragmentation in MCF-7 cells, compared with vehicle-treated cells. The amount of fragmented DNA was determined with the diphenylamine reaction (mean \pm S.D., $n = 4$). (B) Analysis of cell death type (apoptosis and necrosis) in MCF-7 cells treated with the test extract or compounds, at their respective IC_{50} value, or with TRAIL (80 ng/ml), for 12 h as monitored by ethidium bromide/acridine orange staining (mean \pm S.D., $n = 4$). Percentages are based on the total number of dead cells (living cells were excluded).

Apoptosis and necrosis

To investigate the type of cell death – apoptosis or necrosis – induced in MCF-7 cells after treatment with the extract and the isolated compounds, we used acridine orange/ethidium bromide staining to distinguish between apoptotic, necrotic, and viable cells. In untreated cells the range of apoptotic and necrotic cell numbers was 4–8% and 1–4%, respectively. On the other hand, compounds **1** and **3** caused a significant dose-dependent induction of apoptosis ($P < 0.01$ and $P < 0.05$, respectively), where the cells had mainly condensed chromatin, and there was a low percentage of necrotic cells (Fig. 3B). In contrast, treatment of MCF-7 cells with the extract at the concentration of the IC_{50} value significantly induced necrosis ($P < 0.01$) (Fig. 3B). The results were compared to those obtained by treatment with TRAIL, a potent inducer of apoptosis ($P < 0.001$).

Death receptors

Apoptosis or programmed cell death is a common property of multicellular organisms (Danial and Korsmeyer, 2004). It can be triggered by a number of factors, including UV- or γ -irradiation, chemotherapeutic drugs, or signaling by death receptors (DR). The DR family is part of the tumour necrosis factor (TNF) receptor super family (Bhardwaj and Aggarwal, 2003). Triggering members of the DR family by death ligands results in the transduction of either apoptotic or survival signals. Eight members of the DR family have been characterized so far, two of them are TNF-related apoptosis-inducing ligand receptor 1 (TRAILR1, known as DR4) and 2 (TRAILR2, known as DR5) (French and Tschopp, 2003; Wajant, 2003). When these receptors are triggered by corresponding ligands, a number of molecules are recruited to the death domain (DD), and subsequently a signaling cascade is activated. Death ligands also interact with decoy receptors (DcRs) that do not possess DDs and so cannot form signaling complexes. Two types of DR signaling complexes can be distinguished. One of these groups comprises the death-inducing signaling complexes (DISCs) that are formed between the CD95 receptor, DR4, and DR5 (Peter and Kramer, 2003). Due to the promising activities of compounds **1** and **3** as apoptosis-inducing cytotoxic agents, we investigated the possible involvement

of the death receptors DR4 and DR5 and the caspase-8 activation in their apoptotic effect. The findings revealed that compound **1** dramatically enhanced the DR4 and DR5 levels in MCF-7 cells in a highly significant manner ($P < 0.01$), similarly compound **3** significantly induced the DR4 ($P < 0.01$) and DR5 ($P < 0.05$) levels (Fig. 4A).

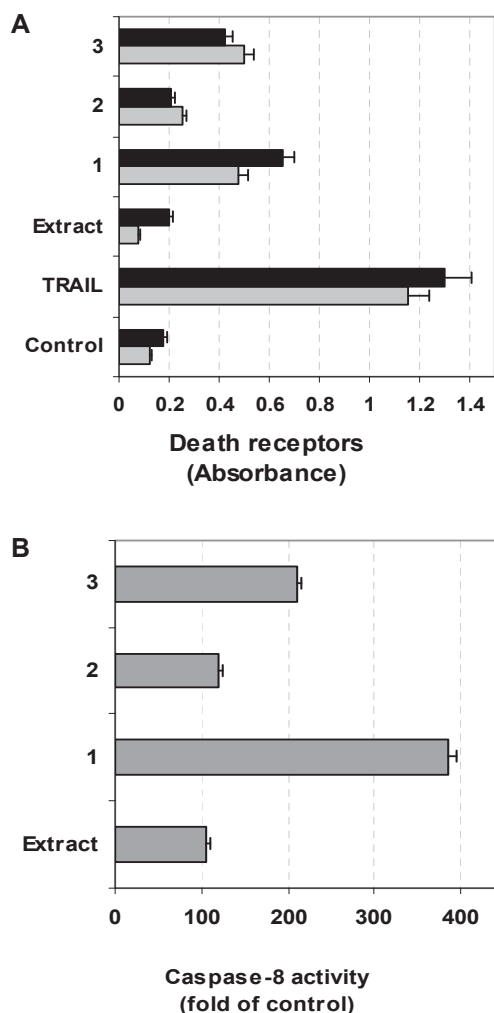


Fig. 4. (A) Effect of test compounds on the activity of death receptors; DR4 (grey bars) and DR5 (black bars) in MCF-7 cells after 12 h of incubation with the compounds, at their respective IC_{50} values, or with TRAIL (80 ng/ml), as assayed by direct ELISA. Data are presented as the absorbance at 450 nm (mean \pm S.D., $n = 4$). (B) Effect of test compounds on the activity of caspase-8 in MCF-7 cells after 12 h of incubation with the compounds at their IC_{50} values. Data are presented as fold of control (mean \pm S.D., $n = 4$).

Caspase-8

DISC formation results in the activation of caspase-8, which plays the central role in transduction of the apoptotic signal. Activation of procaspase-8 is believed to follow an 'induced proximity' model, in which high local concentrations of procaspase-8 at the DISC lead to its autoproteolytic activation, a multi-step cleavage process resulting in the formation of a caspase-8 heterotetramer (Lavrik *et al.*, 2005). This is then released into the cytosol to propagate the apoptotic signal. DcRs can compete with DRs for ligand binding, and the FLICE inhibitory protein (FLIP) blocks procaspase-8 activation at the DISC. Further downstream, inhibitors of apoptosis (IAPs) inhibit effector caspase activation (Lavrik *et al.*, 2005). The treatment of MCF-7 cells with the compounds at their respective IC_{50} values revealed that there was a significant increase in the caspase-8 activity level ($P < 0.01$), when treated with either compound **1** or **3** (Fig. 4B).

Ursolic acid (UA) (**3**) is a pentacyclic triterpenoid found in rosemary and holy basil (Prasad *et al.*, 2011). UA has been found to potentiate TRAIL-induced apoptosis in cancer cells. UA downregulated cell survival proteins and induced the cell surface expression of both TRAIL receptors, DR4 and DR5, and also decreased the expression of the c-Jun N-terminal kinase (JNK) of decoy receptor 2 (DcR2), but not of DcR1. Induction of DRs, however, was dependent on JNK, because UA induced JNK (Prasad *et al.*, 2011). These results are in strong agreement with our results. Additionally, a recent report revealed that UA decreased cell viability and MMP in a dose-dependent manner and increased DNA fragmentation in human liver Hep-G2, Huh7, and Hep3B cell lines (Yan *et al.*, 2010). In Huh7 cells, UA elevated the caspase-3 and caspase-8 activities (Cascon and Brown, 1972). These results are in agreement with our results concerning MCF-7 cells.

According to our knowledge, there has been no previous report on the biological activity of either cabralealactone 3-acetate-24-methyl ether (**1**) or cabralealactone 3-acetate (**2**). Although the only structural difference between these two compounds is the presence of the methyl ether function at C-24 in **1** instead of a carbonyl group in **2**, this difference resulted in a promising antitumour activity of cabralealactone 3-acetate-24-methyl

ether against MCF-7 cells, which was associated with the activation of caspase-8, induction of the death receptors DR4 and DR5, DNA fragmentation, and apoptosis.

Material and Methods

General

For column chromatography (CC), silica gel 60 (0.040–0.063 mm; Merck, Darmstadt, Germany), polyamide 6 (50–160 μm ; Riedel de Haen AG, Seelze, Germany), and Sephadex LH-20 (Pharmacia Fine Chemicals, Uppsala, Sweden) were used. Thin-layer chromatography (TLC) was carried out using silica gel 60 F254 plates (Merck); chromatograms were visualized under UV light at 240 and 366 nm and sprayed with acidic vanillin reagent (Aldrich, St. Louis, MO, USA). Optical rotations were measured on a Jasco (Easton, MD, USA) P-1020 polarimeter, and ^1H NMR spectra on a Varian Unity Inova (Vernon Hills, IL, USA) 400 (400 MHz) and ^{13}C NMR spectra on a Varian Unity 400 (100 MHz) instrument at the Institute of Pharmaceutical Sciences, Graz University, Graz, Austria. The chemical shifts are given in δ (ppm) relative to tetramethylsilane (Me_4Si). Electron impact (EI, 70 eV) mass spectra were recorded on a Waters (Milford, MA, USA) GCT Premier instrument equipped with direct insertion (DI). MALDI-TOF mass spectrometry was performed on a Micromass (Warrington, UK) ToFSpec 2E time-of-flight mass spectrometer at the Institute of Chemical Technology of Organic Materials, Erzherzog-Johann University, Graz, Austria.

Plant material

Fruits of *Forsythia koreana* Nakai were purchased from the Gyung Dong herbal drug market (Seoul, Korea) and identified by faculty members of the Department of Forest Products, Kookmin University, Seoul, Korea. A voucher specimen (YKP04-624) has been deposited in the herbarium of this department.

Extraction and isolation

The dried and powdered fruits of *F. koreana* (1 kg) were extracted with 70% methanol in H_2O (v/v) for 72 h at room temperature. The combined extracts were concentrated at 40 $^\circ\text{C}$ under reduced pressure to give a residue of 22 g which

was re-dissolved in water and partitioned with EtOAc and *n*-BuOH. The EtOAc extract was applied to a silica gel column and eluted with *n*-hexane followed by *n*-hexane/EtOAc mixtures of increasing polarity to yield four main fractions. These fractions were repeatedly chromatographed on preparative silica gel to yield cabralealactone 3-acetate (**2**; 21 mg, $\text{CH}_2\text{Cl}_2/\text{MeOH}$, 99.5:0.5), cabralealactone 3-acetate-24-methyl ether (**1**; 18 mg, $\text{CH}_2\text{Cl}_2/\text{MeOH}$, 99:1), ursolic acid (**3**; 6 mg, $\text{CH}_2\text{Cl}_2/\text{MeOH}$, 98:2), arctigenin (**4**; 12 mg, $\text{CH}_2\text{Cl}_2/\text{MeOH}$, 80:20), arctiin (**5**; 7 mg, $\text{CH}_2\text{Cl}_2/\text{MeOH}/\text{H}_2\text{O}$, 4.5:1:0.1), phillyrin (**6**; 11 mg, $\text{CH}_2\text{Cl}_2/\text{MeOH}/\text{H}_2\text{O}$, 4.5:1:0.1). The aqueous fraction containing compound rutin (**7**; 17 mg) was purified on a polyamide column eluted with water and $\text{H}_2\text{O}/\text{MeOH}$. Compounds caffeic acid (**8**; 4.8 mg) and rosmarinic acid (**9**; 8.7 mg) were detected as blue spots on paper chromatograms and isolated from this fraction by preparative paper chromatography (Whatman 3 MM) using BAW [*n*-BuOH/acetic acid/ H_2O , 3:4:5 (v/v/v), upper phase]. Sephadex LH-20 was used for the final purification of all isolated compounds using methanol as eluent.

Cabralealactone 3-acetate-24-methyl ether (**1**): White powder. – $[\alpha]_{\text{D}}^{+82}$ (c 0.1, CHCl_3). – HREI-MS: $m/z = 474.3688$, calcd. for $\text{C}_{30}\text{H}_{50}\text{O}_4$, 459.3497 (M– CH_3), 442.3459 (M– CH_3OH). – IR: $\nu_{\text{max}} = 3452, 2875, 1746$ (ester CO), 1451, 1371, 1248, 1142 cm^{-1} . – ^1H and ^{13}C NMR: see Table I.

Cabralealactone 3-acetate (**2**): White powder. – $[\alpha]_{\text{D}}^{+46}$ (c 0.1, CHCl_3). – +ESI-MS: $m/z = 469$ $[\text{M}+\text{Na}]^+$. – ^1H and ^{13}C NMR: see Table I.

Cell culture

Three human cell lines were used in testing the anticancer activity including: hepatocellular carcinoma (Hep-G2), breast adenocarcinoma (MCF-7), and colon carcinoma (HCT-116) (ATCC, Manassas, VA, USA), in addition to primary rat splenocytes. Cells were routinely cultured in DMEM (Dulbecco's Modified Eagle's medium) at 37 $^\circ\text{C}$ in humidified air containing 5% CO_2 . Media were supplemented with 10% fetal bovine serum (FBS), 2 mM L-glutamine containing 100 units/ml penicillin G sodium, 100 units/ml streptomycin sulfate, and 250 ng/ml amphotericin B. Monolayer cells were harvested by trypsin/EDTA treatment. The compound to be tested was dissolved in dimethyl sulfoxide (DMSO, 99.9%, HPLC grade) and diluted 1000-fold in the assays. Cells

treated with 0.1% DMSO only were used as controls. Compound dilutions were tested before assays for endotoxin using the Pyrogen[®] Ultra gel clot assay, and were found to be endotoxin-free. All experiments were repeated four times, unless mentioned otherwise, and data are presented as the mean \pm S.D. Unless specifically mentioned, all culture material was obtained from Cambrex Bio-Science (Copenhagen, Denmark), and all chemicals were from Sigma (St. Louis, MO, USA).

Cytotoxicity assay

The cytotoxic effect of the test samples against different solid tumour cell lines was investigated by the 3-(4,5-dimethyl-2-thiazolyl)-2,5-diphenyl-2*H*-tetrazolium bromide (MTT) assay (Messmer *et al.*, 1998). In this assay the yellow tetrazolium salt of MTT is reduced by mitochondrial dehydrogenases in metabolically active cells to form insoluble purple formazan crystals, which are solubilized by the addition of a detergent. Cells ($5 \cdot 10^4$ cells/well) were incubated for 48 h with various concentrations of the test samples (0–50 $\mu\text{g/ml}$) at 37 °C in a FBS-free medium, before subjected to the MTT assay. The absorbance was measured with an ELISA reader (Bio-Rad, Munich, Germany) at 570 nm. The relative cell viability was determined by the amount of MTT converted to the insoluble formazan salt. The data are expressed as the mean percentage of viable cells relative to the respective control cultures treated with the solvent. The cytotoxicity of the sample was compared with that of the known anticancer drug paclitaxel. The half maximal growth inhibitory concentrations (IC₅₀ values) were calculated from the line equation of the dose-dependent curve of each compound.

Apoptosis and necrosis staining

The type of the cell death in the MCF-7 cells was investigated in the treated and untreated cells using acridine orange/ethidium bromide staining. In brief, the cells were placed on glass slides and treated with the IC₅₀ value of the respective compound for 12 h. A mixture of 100 $\mu\text{g/ml}$ each of acridine orange and ethidium bromide was prepared in phosphate buffered saline (PBS). Uptake of the stain by the cells was monitored under a fluorescence microscope, and the apoptotic, necrotic, and viable cells were counted. Acridine orange is taken up by both viable and nonviable

cells and emits a green fluorescence when intercalated into double-stranded nucleic acid (DNA), or red fluorescence when bound to single-stranded nucleic acid (RNA). Ethidium bromide is taken up only by nonviable cells and emits red fluorescence upon intercalation into DNA. We distinguished four types of cells according to the fluorescence emission and the morphological aspect of chromatin condensation in the stained nuclei. (1) Viable cells have uniform bright green nuclei with organized structure. (2) Early apoptotic cells (which still have intact membranes but have started to undergo DNA cleavage) have green nuclei, but perinuclear chromatin condensation is visible as bright green patches or fragments. (3) Late apoptotic cells have orange to red nuclei with condensed or fragmented chromatin. (4) Necrotic cells have uniformly orange to red nuclei with organized structure (Baskic *et al.*, 2006). For apoptotic cell count presentation, we counted cells in both early and late apoptosis.

DNA fragmentation

MCF-7 cells were treated with 30% of the IC₅₀ value of the respective compound for 24 h. DNA fragmentation was essentially assayed as reported previously (Burton, 1956). Briefly, the pellets of the treated and untreated MCF-7 cells were re-suspended in TE buffer (250 μl 10 mM Tris, 1 mM EDTA, pH 8.0) and incubated with an additional volume of lysis buffer (5 mM Tris, 20 mM EDTA, pH 8.0, 0.5% Triton X-100) for 30 min at 48 °C. After lysis, the intact chromatin (pellet) was separated from DNA fragments (supernatant) by centrifugation for 15 min at 13,000 \times g. Pellets were re-suspended in 500 μl TE buffer, and samples were precipitated by adding 500 μl of 10% trichloroacetic acid at 48 °C. Samples were pelleted at 4,000 \times g for 10 min and the supernatant was removed. After addition of 300 μl of 5% trichloroacetic acid, samples were boiled for 15 min. DNA contents were quantified using the diphenylamine reagent (Burton, 1956). The percentage of fragmented DNA was calculated as the ratio of the DNA content in the supernatant to the amount in the pellet.

Death receptor levels

The cells were incubated with the IC₅₀ value of the respective compound for 12 h or with TRAIL (80 ng/ml). MCF-7 cells ($2 \cdot 10^6$) were

lysed after various treatments, and the supernatants (50 μ l/well) were coated onto a 96-well flat bottom microtiter plate (Greiner Labortechnik, Kremsmunster, Austria) in diluent and incubated for 1 h at 37 °C, then overnight at 4 °C, in a humidified chamber. Plates were washed three times with washing buffer [PBS/0.05% polyoxyethylene-20 (Tween-20)], blocked with blocking buffer (PBS/0.05% Tween-20/5% FBS), and incubated at 37 °C for 1.5 h. The plates were washed three times with washing buffer and incubated with the diluted primary antibody (anti-DR4 or anti-DR5) for 1 h at 37 °C. The plates were washed, and diluted second biotin-labeled antibody was added for 1 h at 37 °C. After washing, 50 μ l/well of 1:10,000 diluted peroxidase-conjugated streptavidin (Jackson ImmunoResearchLab., West Grove, PA, USA) was added to each well, and incubated for 1 h at 37 °C. After washing, 50 μ l/well of substrate solution [equal volumes of 3,3',5,5'-tetramethyl benzidine (TMB; 0.4 g/l) and 0.02% H₂O₂ in citric acid buffer] was added. Colour development was stopped by the addition of 50 μ l/well of stopping buffer (1 M HCl) (Surechern Products, Needham Marker, Suffolk, England). Colour intensity was measured at 450 nm using a microplate reader FLUOstar OPTIMA (BMG LABTECH, Offenburg, Germany). The ELISA reader controlling software (Softmax, Sunnyvale, CA, USA) readily processes the digital data of raw absorbance values into a standard

curve from which the TNF- α concentration of unknown samples can be derived directly.

Evaluation of caspase-8 activity

MCF-7 cells ($2 \cdot 10^6$) were lysed after the respective treatments, and the supernatants were incubated with the fluorescent substrate Ac-IETD-fac (Clontech Laboratories, Mountain View, CA, USA) for determination of the caspase-8 activity. Results were obtained using a spectrophotometer (TopCount; Tecan, San Jose, CA, USA) with excitation at 400 nm and emission at 505 nm. A comparison between the fluorescence readings of the treated sample and the untreated cells allows determination of the fold increase.

Statistical analysis

All values are expressed as the mean \pm S.D. of four measurements. Data were statistically analysed using the Statistical Package for Social Scientists (SPSS) 10.00 for windows (SPSS Inc., Chicago, USA). The student's unpaired t-test as well as the one-way analysis of variance (ANOVA) test were used to detect the statistical significance.

Acknowledgement

This work was financially supported by the National Research Center, Cairo, Egypt.

- Bae K. (2000), Medicinal Plants of Korea. Kyo-Hak Publishing Co., Seoul, pp. 399–403.
- Baskic D., Popovic S., Ristic P., and Arsenijevic N. N. (2006), Analysis of cycloheximide-induced apoptosis in human leukocytes: Fluorescence microscopy using annexin V/propidium iodide versus acridine orange/ethidium bromide. *Cell Biol. Int.* **30**, 924–932.
- Bhardwaj A. and Aggarwal B. B. (2003), Receptor-mediated choreography of life and death. *J. Clin. Immunol.* **23**, 317–332.
- Burton K. (1956), A study of the conditions and mechanisms of the diphenylamine reaction for the estimation of deoxyribonucleic acid. *Biochem. J.* **62**, 315–323.
- Cascon S. C. and Brown Jr. K. S. (1972), Biogenetically significant triterpenes in a species of Meliaceae: *Cabralea polytricha* A. Juss. *Tetrahedron* **28**, 315–323.
- Choi I. Y., Moon P. D., Koo H. N., Myung N. Y., Kim S. J., Lee J. Y., Han S. H., Moon G., Seo S. Y., and Sung H. J. (2007), Observations of *Forsythia koreana* methanol extract on mast cell-mediated allergic reactions in experimental models. *In vitro Cell Dev. Biol. Anim.* **43**, 215–221.
- Danial N. N. and Korsmeyer S. J. (2004), Cell death: critical control points. *Cell* **116**, 205–219.
- El-Desouky S. K. and Kim Y.-K. (2008), A phenylethanoid glycoside and other constituents from the fruits of *Forsythia koreana*. *Z. Naturforsch.* **63b**, 90–94.
- Fattorusso R., Frutos S., Sun X., Sucher N. J., and Pellicchia M. (2006), Traditional Chinese medicines with caspase-inhibitory activity. *Phytomedicine* **13**, 16–22.
- French L. E. and Tschopp J. (2003), Protein-based therapeutic approaches targeting death receptors. *Cell Death Differ.* **10**, 117–123.
- Jung H. W., Mahesh R., Lee J. G., Lee S. H., Kim Y. S., and Park Y.-K. (2010), Pinoresinol from the fruits of *Forsythia koreana* inhibits inflammatory respons-

- es in LPS-activated microglia. *Neurosci. Lett.* **480**, 215–220.
- Kalka K., Ahmad N., Criswell T., Boothman D., and Mukhtar H. (2000), Up-regulation of clusterin during phthalocyanine 4 photodynamic therapy mediated apoptosis of tumor cells and ablation of mouse skin tumors. *Cancer Res.* **60**, 5984–5987.
- Kim J. H. and Lee C. H. (2009), Rengyolone inhibits apoptosis *via* etoposide-induced caspase down regulation. *J. Microbiol. Biotechnol.* **19**, 286–290.
- Kim N. Y., Kang T. H., Song E. K., Pae H. O., Chung H. T., and Kim Y. C. (2000), Inhibitory effects of butanol fraction of the aqueous extract of *Forsythia koreana* on the nitric oxide production by murine macrophage-like RAW 264.7 cells. *J. Ethnopharmacol.* **73**, 323–327.
- Kitagawa S., Tsukamoto H., Hisada S., and Nishibe S. (1984a), Studies on the Chinese crude drug *Forsythia fructus*. *Chem. Pharm. Bull.* **32**, 1209–1213.
- Kitagawa S., Hisada S., and Nishibe S. (1984b), Phenolic compounds from *Forsythia* leaves. *Phytochemistry* **32**, 1635–1636.
- Kitagawa S., Nishibe S., and Baba H. (1987), Studies on the Chinese crude drug “*Forsythia fructus*”. VIII. On isolation of phenylpropanoid glycosides from fruits of *Forsythia koreana* and their antibacterial activity. *Yakugaku Zasshi* **107**, 274–278.
- Kong X. T., Fang H. T., Jiang G. Q., Zhai S. Z., O’Connell D. L., and Brewster D. R. (1993), Treatment of acute bronchiolitis with Chinese herbs. *Arch. Dis. Child.* **68**, 468–471.
- Lavrik I., Golks A., and Kammer P. (2005), Death receptor signaling. *J. Cell Sci.* **118**, 265–267.
- Lee J. S., Min B. S., and Bae K. W. (1996), Effects of *Forsythia fructus* on L1210 and HL-60 cells. *Yakhaka Hoeji* **40**, 462–467.
- Lee J. Y., Cho B. J., Park T. W., Park B. E., Kim S. J., Sim S. S., and Kim C. J. (2010), Dibenzylbutyrolactone lignans from *Forsythia koreana* fruits attenuate lipopolysaccharide-induced inducible nitric oxide synthetase and cyclooxygenase-2 expressions through activation of nuclear factor- κ B and mitogen-activated protein kinase in RAW 264.7 cells. *Biol. Pharm. Bull.* **33**, 1847–1853.
- Messmer U. K., Reed U. K., and Brüne B. (1998), Bcl-2 protects macrophages from nitric oxide-induced apoptosis. *J. Biol. Chem.* **271**, 20192–20197.
- Nishibe S. (2002), The plant origins of herbal medicines and their quality evaluation. *Yakugaku Zasshi* **122**, 363–379.
- Peter M. E. and Krammer P. H. (2003), The CD95 (APO-1/Fas) DISC and beyond. *Cell Death Differ.* **10**, 26–35.
- Prasad S., Yadav V. R., Kannappan R., and Aggarwal B. B. (2011), Ursolic acid, a pentacyclin triterpene, potentiates TRAIL-induced apoptosis through p53-independent up-regulation of death receptors: evidence for the role of reactive oxygen species and JNK. *J. Biol. Chem.* **286**, 5546–5557.
- Rao M. M., Meshulam H., Zelink R., and Lavie D. (1975), *Cabralea eichleriana* dc. (Meliaceae) – I. Structure and stereochemistry of wood extractives. *Tetrahedron* **31**, 333–339.
- Seebacher W., Simic N., Weis R., Saf R., and Kunert O. (2003), Complete assignments of ^1H and ^{13}C resonances of oleanolic acid, 18 α -oleanolic acid, ursolic acid and their 11-oxo derivatives. *Magn. Reson. Chem.* **41**, 636–638.
- Vuorela P., Leinonen M., Saikku P., Tammela P., Rauha J. P., Wennberg T., and Vuorela H. (2004), Natural products in the process of finding new drug candidates. *Curr. Med. Chem.* **11**, 1375–1389.
- Wajant H. (2003), Death receptors. *Essays Biochem.* **39**, 53–71.
- Yan S. L., Huang C. Y., Wu S. T., and Yin M. C. (2010), Oleanolic acid and ursolic acid induce apoptosis in four human liver cancer cell lines. *Toxicol. In Vitro* **24**, 842–848.